Inorganic Chemistry

Article

pubs.acs.org/IC

# Photophysical Processes in Rhenium(I) Diiminetricarbonyl Arylisocyanides Featuring Three Interacting Triplet Excited States

Joseph M. Favale, Jr., Evgeny O. Danilov, James E. Yarnell, and Felix N. Castellano*

Department of Chemistry, North Carolina State University (NCSU), Raleigh, North Carolina 27695-8204, United States

Supporting Information

**ABSTRACT:** We present a series of four transition-metal complexes based on the rhenium(I) tricarbonyl 1,10-phenanthroline (phen) template, with a lone ancillary arylisocyanide (CNAr) ligand to yield metal−organic chromophores of the generic molecular formula $[Re(phen)(CO)_3(CNAr)]^+$ [CNAr = 2,6-diisopropylphenyl isocyanide (**1**), 4-phenyl-2,6-diisopropylphenyl isocyanide (**2**), 4-phenylethynyl-2,6-diisopropylphenyl isocyanide (**3**), and 4-biphenyl-2,6-diisopropylphenyl isocyanide (**4**)]. This particular series features varied degrees of $\pi$-conjugation length in the CNAr moiety, resulting in significant modulation in the resultant photophysical properties. All molecules possess long-lived [8−700 $\mu$s at room temperature (RT)], strongly blue-green photoluminescent and highly energetic excited states ($\lambda_{max,em}$ = 500−518 nm; $\delta$ = 14−64%). Each of these chromophores has been photophysically investigated using static and dynamic spectroscopic techniques, the latter probed from ultrafast to supra-nanosecond time scales using transient absorption and photoluminescence (PL). Time-resolved PL intensity decays recorded as a function of the temperature were consistent with the presence of at least two emissive states lying closely spaced in energy with a third nonemissive state lying much higher in energy and likely ligand-field in character. The combined experimental evidence, along with the aid of electronic structure calculations (density functional theory and time-dependent density functional theory performed at the M06/Def2-SVP/SDD level), illustrates that the CNAr ligand is actively engaged in manipulating the excited-state decay in three of these molecules (**2**−**4**), wherein the triplet metal-to-ligand charge-transfer ($^3$MLCT) state along with two distinct triplet ligand-centered ($^3$LC) excited-state configurations (phen and CNAr) conspire to produce the resultant photophysical properties. Because the $\pi$ conjugation within the CNAr ligand was extended, an interesting shift in the dominant photophysical processes was observed. When the CNAr conjugation length is short, as in **1**, the phenanthroline $^3$LC state dominates, resulting in a configurationally mixed triplet excited state of both LC and MLCT character. With more extended $\pi$ conjugation in the CNAr subunit (**2**−**4**), the initially generated $^3$LC(phen)/$^3$MLCT excited state ultimately migrates to the CNAr $^3$LC state on the order of tens of picoseconds. Molecules **3** and **4** in this series also feature unique examples of inorganic excimer formation, as evidenced by dynamic self-quenching in the corresponding PL intensity decays accompanied by the observation of a short-lived low-energy emission feature.

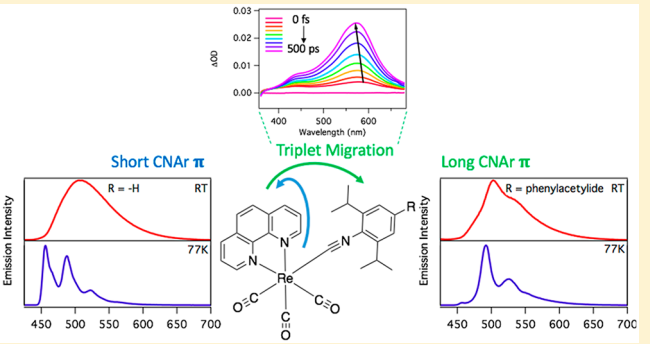


## INTRODUCTION

For approximately 4 decades, *fac*-rhenium(I) diiminetricarbonyl complexes have drawn considerable attention and experimental investigation.[1−15] These chromophores have potential applications in a variety of photonics-relevant technologies including solar energy conversion, photochemical transformations, photocatalytic carbon dioxide and proton reduction, photoluminescent molecular devices, and photoluminescence (PL) sensing of numerous analytes.[16−29] These attributes result from their low-energy visible-light absorption properties with corresponding long excited-state lifetimes suitable for sensitizing myriad intramolecular and bimolecular electron- and energy-transfer reactions.

Prior investigations have concluded that the vast majority of chromophores in the particular rhenium(I) tricarbonyl family possess lowest-lying excited states, which are predominantly metal-to-ligand charge transfer (MLCT) in nature. This manifests in broad, featureless emission spectra that are highly dependent on environmental factors such as the solvent polarity. It is also possible for low-energy ligand-centered (LC) excited states to be present in these molecules lying in close energetic proximity to the MLCT states. Any possible thermal equilibrium or activation between these closely lying states may lead to beneficial consequences, including dramatic extension of the original MLCT excited-state lifetime. The vast majority of previous studies have focused on tuning of the MLCT states through manipulation of the lowest unoccupied molecular orbital (LUMO) energetics directly resulting from structural modifications in the appended diimine ligand. It is

Received: April 19, 2019





DOI: 10.1021/acs.inorgchem.9b01155
Inorg. Chem. XXXX, XXX, XXX−XXX

**Scheme 1. General Synthetic Pathway and Molecular Structures of the *fac*-Rhenium(I) Complexes 1−4**

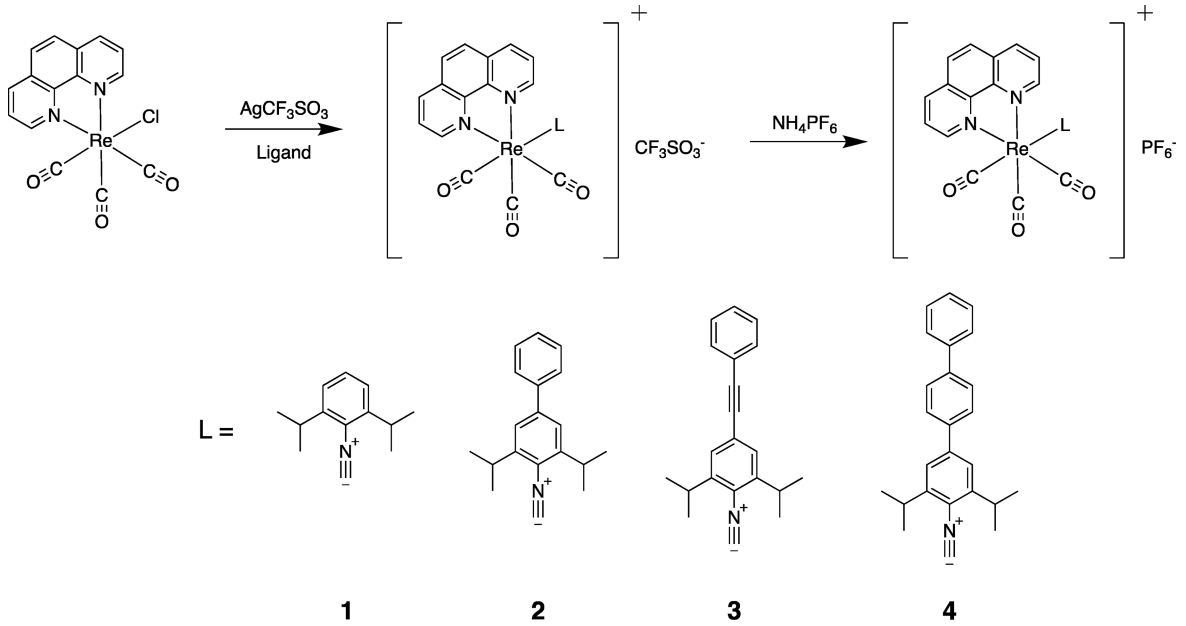


important to note that through temperature-dependent investigations, the proximity and ordering of multiple excited states resident in these chromophores can be readily elucidated.[2,6−8,11,12,14,30]

To date, a variety of ancillary ligands have been incorporated in these rhenium(I) diiminetricarbonyl frameworks to systematically modulate excited-state decay properties, leveraging deterministic energy gap law behavior.[31,32] These ancillary substitutions include the incorporation of halides,[1,3,4] pyridine and piperidine,[2,6,7,11,12] and, of particular significance to the present work, isocyanides.[8,13,33−36] Isocyanide ligands, featuring both alkyl and aryl substituents, serve as strong $\sigma$ donors and good $\pi$ acceptors, similar to that imposed by carbon monoxide (CO).[37−39] Therefore, isocyanides impart a strong ligand field to the rhenium(I) center while offering the opportunity for deliberately installing organic subunits with meaningful variation in their singlet and triplet excited-state energies. Extensive work into perturbation of the photophysical properites of rhenium(I) isocyano complexes has been performed, via substituent modification on simple arylisocyanide (CNAr) ligands and the number of isocyano versus carbonyl ligands on the complex.[33] These studies have found that the photophysical behavior of such complexes is dependent on the d$\pi$(Re)−$\pi\pi^*$(diimine) MLCT, with the electronic influence of the isocyanide playing an ancilliary role in the energetics of this excited state. It is noted that further functionalization of the isocyanide provides a route to a more drastic modification of the properties of these rhenium(I) complexes. Such molecules are potentially valuable for driving catalytic transformations initiated through triplet−triplet energy transfer, as has been recently discovered.[40,41] Beyond rhenium(I) complexes, isocyanide ligands have been employed as ancillary ligands in other photophysically active systems. Most of these are derived from iridium(III) cyclometalate archetypes, and all feature bright phosphorescence across the visible spectrum from a predominantly $^3$LC state, depending on the cyclometalate chosen.[42−46] Further utilization of isocyanides has come in the form of homoleptic complexes of group VI metals, where the isocyanide is the chromophoric ligand and the photophysics are dominated by pure $^3$MLCT.[47−49] because of their utilization primarily as an ancillary ligand, the photophysical properties of lower-energy CNAr moieties have rarely been explored in rhenium(I).

The current work focuses on varying the $\pi$-conjugation length in the ancillary CNAr ligand fused to the rhenium(I) tricarbonyl 1,10-phenanthroline (phen) template to yield metal−organic chromophores of the generic molecular formula [Re(phen)(CO)$_3$(CNAr)]$^+$ (**1**−**4** in Scheme 1) featuring long-lived and highly energetic excited-state properties. All of these molecules have been photophysically investigated using static and dynamic spectroscopic techniques, the latter probed from ultrafast to suprananosecond time scales using transient absorption (TA) and PL. Electronic structure calculations utilizing density functional theory (DFT) and time-dependent DFT (TD-DFT) methods have been performed on this series of chromophores to support the experimental spectroscopic assignments. The combined experimental and computational evidence illustrates that the CNAr subunit in **2**−**4** was actively engaged in manipulating the excited-state decay in these molecules, wherein the $^3$MLCT and two distinct $^3$LC excited-state configurations (phen and CNAr) conspire to produce the resultant photophysical properties.

## RESULTS AND DISCUSSION

**Syntheses.** The rhenium(I) complexes **1**−**4** were synthesized using the general procedure outlined in Scheme 1. Each of the isocyanide ligands was prepared following the general synthetic procedure outlined in Figures S1−S3. Each of the target compounds was purified through multiple precipitations by dissolving the isolated product in methanol, followed by treatment with aqueous $NH_4PF_6$. The final rhenium(I) complexes were structurally characterized using $^1$H and $^{13}$C NMR spectroscopy, high-resolution time-of-flight electrospray ionization mass spectrometry (ESI-MS), and Fourier transform infrared (FTIR) spectroscopy. The purified molecules were determined to be both thermally and photochemically stable in nonhalogenated solvents, with a minor degree of photodegradation observed in halogenated solvents upon extended


DOI: 10.1021/acs.inorgchem.9b01155
Inorg. Chem. XXXX, XXX, XXX−XXX

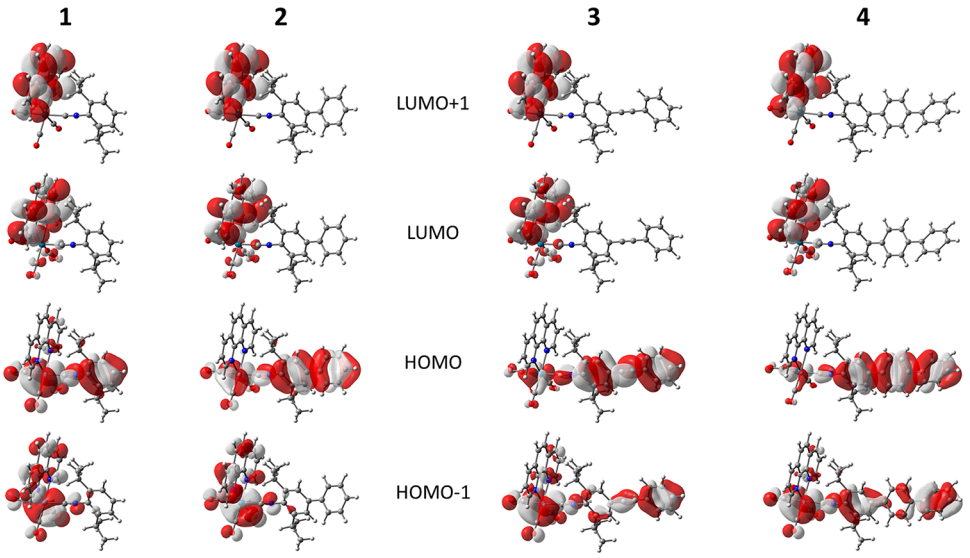


**Figure 1.** Frontier molecular orbitals for **1**−**4**. Calculations were performed at the DFT//M06/Def2-SVP/SDD level of theory.

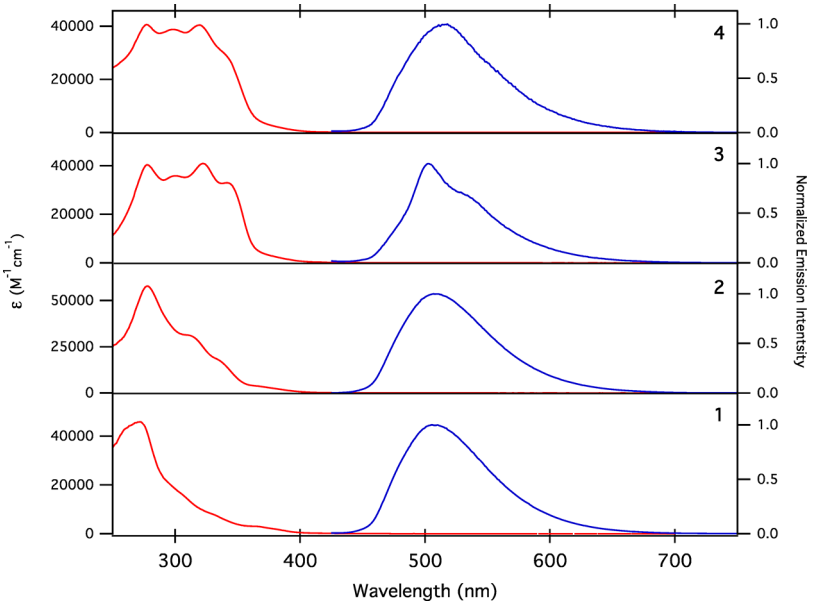


**Figure 2.** Electronic UV−vis absorption (red) and normalized static PL (blue) spectra of **1**−**4** in THF at RT. The PL spectra were recorded with samples having an o.d. = 0.1 at 355 nm excitation in deoxygenated THF.

light exposure. The new molecules are soluble in a variety of polar organic solvents, and tetrahydrofuran (THF) was selected as the solvent medium for all spectroscopic measurements in this contribution.

**Electronic Structure Calculations.** Prior to the discussion of the photophysical properties of complexes **1**−**4**, a brief DFT-based analysis is presented. The DFT and TD-DFT calculations were performed at the M06/Def2-SVP/SDD level of theory using the polarizable continuum model (PCM) to simulate the THF solvent environment. The ground-state structures for **1**−**4** were optimized, and the frontier molecular orbitals are presented in Figure 1 and the resulting energies collected in Table S1. In all four molecules, LUMO and LUMO+1 are the in-phase and out-of-phase $\pi^*$-orbital combinations, respectively, localized on the phen ligand. The energies of LUMO (−3.080 to −3.089 eV) and LUMO+1 (−2.865 to −2.872 eV) are also consistent across the series, demonstrating that modification of the ancillary isocyanide ligand does not significantly impact the electronic structure of the phen ligand. The highest occupied molecular orbital (HOMO) for these complexes is largely localized on the CNAr ligand, but there is a significant contribution from the Re d orbitals that decreases uponn going from **1** to **4**. The increase in the electronic localization on the isocyanide ligand also correlates with the change in the energy where the HOMO energy increases from −7.274 eV (in **1**) to −6.676 eV (in **4**). HOMO−1 consists largely of Re d orbital contributions with some contribution localized on the phen ligand (**1** and **2**) or the CNAr ligand (**3** and **4**).

**Static Absorption and PL Measurements.** The UV−vis electronic absorption and PL spectra of **1**−**4** measured in THF are presented in Figure 2, with additional information collected in Table 1. In all of the complexes in this study, the red edges of the absorption bands greater than 350 nm have been


DOI: 10.1021/acs.inorgchem.9b01155
Inorg. Chem. XXXX, XXX, XXX−XXX

**Table 1. Static UV−Vis Absorption and PL Data for 1−4 at RT and 77 K[a]**

| complex | Abs $\lambda_{max}$, nm ($\varepsilon$, $M^{-1}$ $cm^{-1}$) | RT PL $\lambda_{max}$, nm | 77 K Em $\lambda_{max}$, nm |
|---|---|---|---|
| **1** | 273 (45700), 305 (16400), 365 (3000) | 505 | 456 |
| **2** | 278 (57900), 315 (30200), 339 (15800), 367 (3600) | 507 | 457 |
| **3** | 278 (40400), 300 (35900), 322 (40900), 341 (33000), 370 (4000) | 503, 535 (sh) | 492 |
| **4** | 277 (40600), 298 (38800), 319 (40500), 340 (29400), 370 (3800) | 518 | 495 |

[a]All RT spectra measured in THF (absorption), deoxygenated THF (PL), and 77 K PL data recorded in Me-THF frozen glasses. All wavelengths measured to ±2 nm.

assigned as charge transfer in character. A previous study by Rillema and co-workers demonstrated that the lowest-energy absorption band on a rhenium(I) complex bearing a 2,6-dimethylphenyl isocyanide was a metal−ligand-to-ligand charge-transfer singlet.[13] The TD-DFT calculations performed here confirm this assignment as the lowest-energy transition in **1**−**4** consisting of a rhenium/isocyanide (metal/ligand)-to-phen ligand charge-transfer transition (Figures S9−S12). However, the oscillator strength of this transition is low, so it likely contributes very little to the experimentally observed red shoulder in the corresponding absorption spectra (Figure 2). When the higher-lying transitions $S_0 \rightarrow S_2$ through $S_0 \rightarrow S_4$ in complexes **1** and **2** are examined, the transition type changes to a Re(d$\pi$) → phen($\pi^*$) MLCT transition with higher oscillator strength, contributing to the observed shoulder in the measured spectra.

The high-energy portion ($\delta$ < 300 nm) of the electronic spectrum of **1** is dominated by phen-based $\pi-\pi^*$ transitions with some $\pi-\pi^*$ contribution from the isocyanide ligand. The increased oscillator strength of the spectral features observed between 300 and 350 nm when moving across the series is attributed to the presence of additional aromatic rings on the isocyanide ligands because extension of the $\pi$ system lowers the energy while raising the oscillator strength of the LC $\pi-\pi^*$ transitions localized on the isocyanide ligand. Experimentally, this results in the red shift and broadening of the main absorption band in the electronic spectra.

The static PL spectra for **1** and **2** measured in THF are broad and featureless and are also highly quenched by dissolved oxygen, suggesting significant triplet excited-state character in the PL emission; all of these observations are consistent with some degree of charge-transfer character. We note that simple visual inspection of the RT PL spectra in these molecules can be misleading because multiple closely lying excited states each contribute PL intensity proportional to their respective radiative rate constant.[8] Therefore, unambiguous identification of the lowest excited state requires more sophisticated spectroscopic examination as described below.

The structured PL spectra exhibited by **3** and **4** (Figure 2) at room temperature (RT) in THF immediately suggest interactions between multiple excited states in close energetic proximity. Here, **3** exhibits the most obvious vibronic components, whereas **4** features much more subtle broadening and shouldering toward lower emission energies. All PL spectral features in both **3** and **4** are strongly quenched by dissolved oxygen in THF solutions. This oxygen quenching was found to be asymmetric over the entire emission envelope, with the higher-energy emission more strongly quenched than the lower-energy region. Given these initial steady-state spectroscopic observations, the main PL emission features of **3** and **4** are tentatively assigned to a mixture of $^3$LC and $^3$MLCT excited states. In addition, the optimized triplet-state spin densities obtained from DFT support this as the localization of the unpaired spins to be localized on the rhenium, the isocyanide, and the phen ligand (Figures S15 and

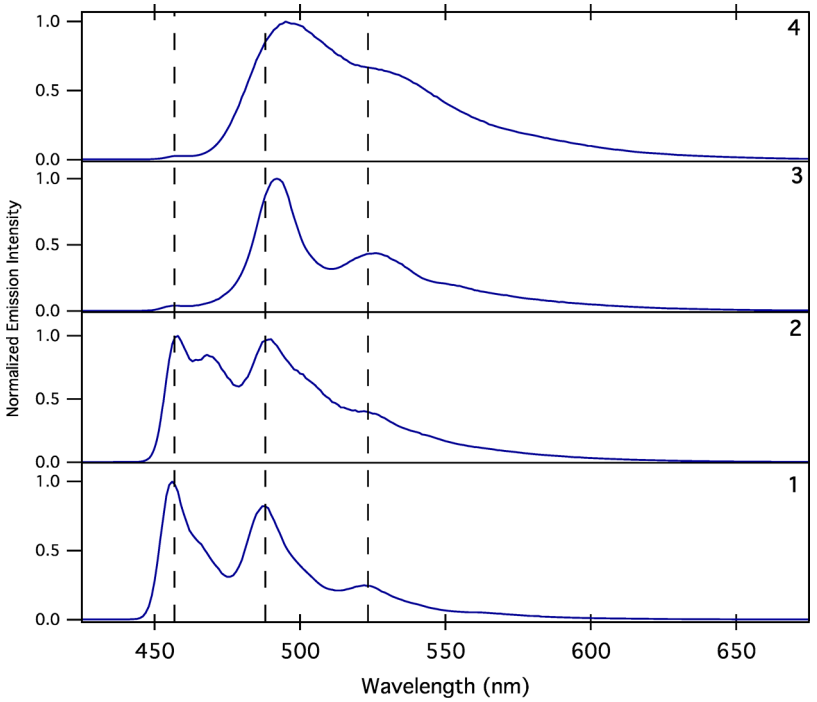


**Figure 3.** Normalized static PL spectra of **1**−**4** measured in 2-MeTHF frozen glasses at 77 K ($\lambda_{ex}$= 355 nm). The vertical dashed lines are drawn as a guide for the eye to illustrate the marked differences in the PL spectral profiles in **1** and **2** with respect to **3** and **4**.


DOI: 10.1021/acs.inorgchem.9b01155
Inorg. Chem. XXXX, XXX, XXX−XXX

S16). Additional static and dynamic experiments described below will help to elucidate the true nature of these excited manifolds and their respective interactions.

The static PL spectra for **1**−**4** were recorded at 77 K in 2-methyltetrahydrofuran (2-MeTHF) glasses following 355 nm excitation (Figure 3). In **1** and **2**, the 77 K PL emission spectra are significantly blue-shifted relative to their corresponding RT spectra recorded in THF and a high degree of vibronic structure also becomes evident. The thermally induced Stokes shifts [$\Delta E_s = E_{00}(77\ K) - E_{00}(298\ K)$] observed in **1** and **2** are quite large and quantitatively identical in magnitude given the 1 nm bandpass of the PL experiments, $\Delta E_s$ = 2128 and 2158 $cm^{-1}$, respectively. By comparison, the $\Delta E_s$ measured for the rhenium(I) diiminetricarbonyl $^3$MLCT model complex Re(phen)$(CO)_3$Cl is 2381 $cm^{-1}$ in the same solvent measured under identical experimental conditions (Figure S17). In all of these instances, the magnitude of the $\Delta E_s$ values remained consistent with that anticipated for strongly polar charge-transfer excited states. However, the measured 77 K PL spectra of **1** and **2** quantitatively align with the $^3$LC phosphorescence measured for phen,[2] indicative of $^3$MLCT/$^3$LC state crossover occurring between RT and 77 K. In essence, the lack of solvent reorganization in the vitrified medium renders the $^3$MLCT state slightly higher in energy with respect to the lower-lying 1,10-phenantholine-centered $^3$LC state. This behavior is analogous to previous work on rhenium(I) diimine complexes containing alkylisocyanide ancillary ligands, in addition to being observed in various MLCT excited states featuring other transition metals.[2,50,51] Of particular relevance to the current observations, the 77 K emission spectrum of $[Ir(phen)_2Cl_2]Cl$ is quantitatively similar to the PL spectrum recorded for **1**, which is also similar to the phosphorescence of free phen.[52]

In **3** and **4**, the static PL emission spectra exhibit substantially smaller thermally induced Stokes shifts ($\Delta E_s$ = 444 and 897 $cm^{-1}$, respectively) in comparison to **1** and **2**, concomitant with the observation of distinct vibronic progressions becoming revealed at 77 K in these molecules (Figure 3). Because the MLCT states are expected to blue shift over 2000 $cm^{-1}$ in these chromophores while the phen-based $^3$LC states remain at much higher energy, this lower-energy phosphorescence emission measured in **3** and **4** must be emanating from a lower-energy triplet excited state. Because molecules **3** and **4** feature aryl-based isocyanide substituents possessing extended $\pi$ conjugation (phenylacetylene and biphenyl, respectively), it immediately becomes apparent that these 77 K PL spectra are most appropriately assigned as the $^3$LC states localized on the CNAr substituents in **3** and **4**. These particular molecules now emerge as quite interesting because they likely feature RT electronic interactions occurring between three distinct triplet excited states, namely, the lowest MLCT state and two low-lying $^3$LC states resident on two distinct chromophoric ligands (phen and CNAr) installed on the same rhenium(I) center. To the best of our knowledge, **3** and **4** represent the first examples of rhenium(I) tricarbonyl chromophores, with three distinct triplet excited states being thermally accessible simultaneously. These interactions will be further elucidated below through temperature-dependent excited-state dynamics.

**Concentration-Dependent Self-Quenching.** Another interesting phenomenon consistently observed in **3** and **4** was a concentration dependence of their excited-state lifetimes in THF. The combined photophysical data measured for **1**−**4** under optically dilute conditions are presented in Table 2. At higher concentrations (>$10^{-5}$ M), the excited-state decay was best fit with a biexponential function in **3** and **4** because there was now clear evidence of an additional emissive species being present in these samples as visualized in static and dynamic PL experiments (Figure 4). Note that no aggregation was observed in the ground states of **3** and **4**, as evidenced by the corresponding electronic absorption spectra being consistent with the Beer−Lambert law over all chromophore concentrations investigated. The static PL emission spectra measured in concentrated samples of **3** and **4** contained a low-energy shoulder; see the solid black lines in Figure 4. In addition, time-resolved PL experiments revealed that both molecules possessed shorter lifetimes than those recorded in the corresponding diluted samples. Therefore, time-gated PL emission spectra were recorded for concentrated samples of **3** and **4** at both short (250 ns) and long (50 $\mu$s) delay times in order differentiate the high- and low-energy features observed in the static PL spectra (Figure 4). The time-gated spectrum recorded for **3** at the 250 ns delay time (solid red line) was very broad in nature, spanning most of the visible region, and featured rather intense emission toward the red region of the

**Table 2. Summary of the Photophysical Parameters of 1−4 Measured in THF at RT**

| complex | $\Phi^a$ | $\tau_{em}$ ($\mu$s) | $\tau_{TA}$ ($\mu$s) | $k_r$ ($\times 10^3$ $s^{-1}$)$^b$ | $k_{nr}$ ($\times 10^3$ $s^{-1}$)$^b$ |
|---|---|---|---|---|---|
| **1** | 0.64 | 8.1 | 8.9 | 72.0 | 40.5 |
| **2** | 0.48 | 14.2 | 15.5 | 31.0 | 33.6 |
| **3** | 0.14 | *d* | 710$^c$ | 0.20 | 1.2 |
| **4** | 0.15 | *d* | 663$^c$ | 0.22 | 1.3 |

$^a$Measured relative to a 9,10-diphenylanthracene standard quantum counter, ±10%.[56] $^b$Values calculated from the PL quantum yield and TA decay lifetime values, ±5%. $^c$Excited-state lifetime extrapolated to infinite dilution, ±5%. $^d$Values could not be accurately determined because of the lower quantum yields and longer lifetimes. Higher concentrations were necessary for an accurate kinetic fit, which ultimately manifested quenched excited-state best fits using biexponential kinetics.

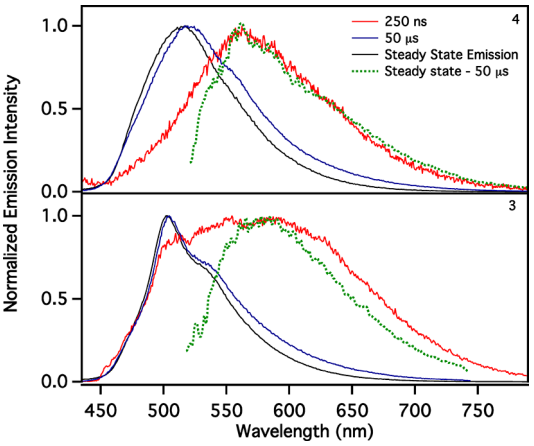


**Figure 4.** Time-gated PL emission spectra recorded for **3** (bottom) and **4** (top) measured in THF using nanosecond laser pulses ($\lambda_{ex}$ = 355 nm; 7 ns fwhm) and ICCD detection. Spectra at 250 ns delay (red), relative to the excitation pulse, recorded with a 50 ns gate width. Spectra at 50 $\mu$s delay (blue) recorded with a 1 $\mu$s gate width. Normalized steady-state PL spectra (black) are shown for comparison along with the static PL spectrum that subtracts the normalized time-resolved PL spectrum recorded at 50 $\mu$s delay.


DOI: 10.1021/acs.inorgchem.9b01155
Inorg. Chem. XXXX, XXX, XXX−XXX

spectrum. The 50 δs delay spectrum in **3** (solid blue line) almost quantitatively reproduced the static PL spectrum at this concentration, which possessed most of the spectral characteristics of the diluted chromophore, as seen in Figure 2. Similar results were obtained in analogous experiments, where **4** was examined under identical experimental conditions.

In both instances, the PL decay at earlier times was dominated by emission emanating from a characteristically distinct species decaying in parallel with the longer-lived bluer species corresponding to the photophysical response from the diluted molecule. Because the shorter-lived PL emission in **3** and **4** was red-shifted, in addition to being broad and featureless, we propose that an excimer-type interaction was responsible for this behavior. The excited-state lifetimes in **3** and **4** are so long-lived (710 and 663 δs, respectively) that this readily enables bimolecular reactions with ground-state molecules, ultimately leading to low-energy excimer formation in a portion of the decaying excited-state population. Although rare, a handful of examples of inorganic triplet excimers have been reported, almost exclusively based on square-planar platinum(II) complexes.[53−55] However, in the current molecules, it is the $^3$LC excited states resident on the CNAr ligands that are deemed responsible for producing the proposed excimers in **3** and **4**. In an attempt to generate the true emission spectral profile of the proposed excimers, the normalized time-gated spectrum at 50 μs was subtracted from the corresponding static spectrum in both **3** and **4** (Figure 4, dashed green lines). It is clear that these difference spectra produce profiles that are substantially red-shifted and distinct of those measured in the diluted molecules, indeed qualitatively consistent with excimer formation. This excimer interaction was also manifested in the static PL emission spectra measured in concentrated solutions of **3** and **4**, where significant amplification of the PL intensity on the red side of the static spectral envelope was clearly observed (Figure S18).

The excited-state decay kinetics was measured as a function of the chromophore concentration in order to use the Stern−Volmer equation to quantify the rate of self-quenching ($k_q$) in **3** and **4** as well as give an estimate of the excited-state lifetime at infinite dilution ($\tau_0$). Figure S19 presents these Stern−Volmer plots, where the $k_q$ values were found to be $8.8 \times 10^8$ and $5.80 \times 10^8$ $M^{-1}$ $s^{-1}$ for **3** and **4**, respectively. Because the extent of orbital overlap in an excimer is related to the relative red shift observed between monomer and excimer emission, **3** is clearly red-shifted with respect to **4**. To rationalize this result, we postulate that the isocyanide ligand in **3** has the potential for greater π overlap between distinct molecules due to the more planar nature of the ethynyl linker used in this instance. In **3**, the red shift was approximately 2766 $cm^{-1}$, while that in **4** was found to be ∼1511 $cm^{-1}$. Overall, the π-conjugated CNAr subunits appear to facilitate intermolecular π stacking during excited-state decay, and it is this interaction that is most likely responsible for excimer formation in **3** and **4**. Moving forward, this suggests a general design strategy in metal−organic chromophores wherein the efficient generation of a long-lived triplet intraligand excited state can lead to entirely new classes of excimer-based PL projecting from the red into the near-IR.

**Excited-State Dynamics.** In order to comprehend the photophysical processes leading to formation of the lowest excited-state configurations in **1**−**4**, ultrafast TA experiments were performed in THF solutions. The TA difference spectra are shown in Figure 4, with the time constants fit to the most prominent signals summarized in Table 3, with kinetic data given in Figures S20 and S21. What becomes immediately apparent is the difference in dynamics between **1** and **2**−**4**. In **1**, there is the prompt (∼200 fs) formation of a broad excited-state absorbance feature traversing most of the visible spectrum. This is followed by very subtle shifts in the signal maximum around 400−450 nm with a corresponding formation time constant of 25 ps (Figure S21). These dynamics differ significantly from those found in the $^3$MLCT model compound $Re(phen)(CO)_3Cl$, whose difference spectrum is presented in Figure 4 at 2.12 ps delay. In our experiments (Figure S22) and previous literature results,[57,58] 100 fs pulsed-laser excitation of $Re(phen)(CO)_3Cl$ results in the nearly prompt formation of its $^3$MLCT excited-state absorption with a maximum near 475 nm, consistent with that shown in Figure 5. This was followed by the growth of a shoulder at 575 nm taking place on the order of tens of picoseconds. The prompt signal has been assigned to rapid dynamics associated with the formation of the phen radical anion along with intersystem crossing to the $^3$MLCT manifold. The longer-time-scale (picosecond) dynamics was assigned to vibrational relaxation occurring within the $^3$MLCT manifold that ultimately produces a transient signal that persists into the nanoseconds time scale, which is the lowest-energy $^3$MLCT excited state. By comparison, the prompt TA signatures measured in **1** on femtosecond-to-nanosecond time scales are clearly inconsistent with the expected salient features of the phen radical anion. Instead, there is a prompt formation of a broad transient absorbance (across most of the visible region) with a discernible peak at 400 nm, which decays away only slightly over the entire length of the delay line (5.5 ns). Because the molecular photophysics from the lowest excited state in **1** and related molecules based on iridium(III) and platinum(II) is considered to be configurationally mixed because of energetically proximate $^3$MLCT and $^3$LC (phen) manifolds,[50,59−63] we assign the TAs observed in **1** to the $^3$phen moiety because the phen radical anion does not contribute significant oscillator strength. In the available published examples of TA studies executed on configurationally mixed excited states, the dominating absorbing species is unequivocally the $^3$LC state in all instances. Similar results have also been echoed in metal−organic molecules featuring triplet excited-state equilibria.[58,64−70]

For **2**−**4**, it is clear that the ultimate triplet excited state formed is significantly different with respect to that measured in **1**, as evidenced by the continued growth in the TA signals on the order of tens of picoseconds. These molecules also possess a similar prompt (130−220 fs) formation of the broad visible absorption signal observed in **1** at both short and long delay times. Combined together, we assign this initial absorption feature in **2**−**4** as resulting from intersystem

**Table 3. Summary of the Time Constants from Ultrafast TA Kinetic Modeling**[a]

| complex | $\lambda_{fit}$ (nm) | $\tau_1$ (fs) | $\tau_2$ (ps) | $\tau_3$ (ps) |
|---|---|---|---|---|
| **1** | 400, 417, 552, 649 | 200 (±50) | 25 (±10) | |
| **2** | 398, 536 | 190 (±50) | 5 (±1) | 50 (±8) |
| **3** | 523, 537, 580 | 130 (±60) | 3.0 (±0.2) | 13.5 (±0.4) |
| **4** | 572, 603 | 220 (±20) | 3.4 (±0.3) | 26 (±1) |

[a]Fits and kinetic data from which these time constants were obtained can be found in Figures SI20 and S21.


DOI: 10.1021/acs.inorgchem.9b01155
Inorg. Chem. XXXX, XXX, XXX−XXX

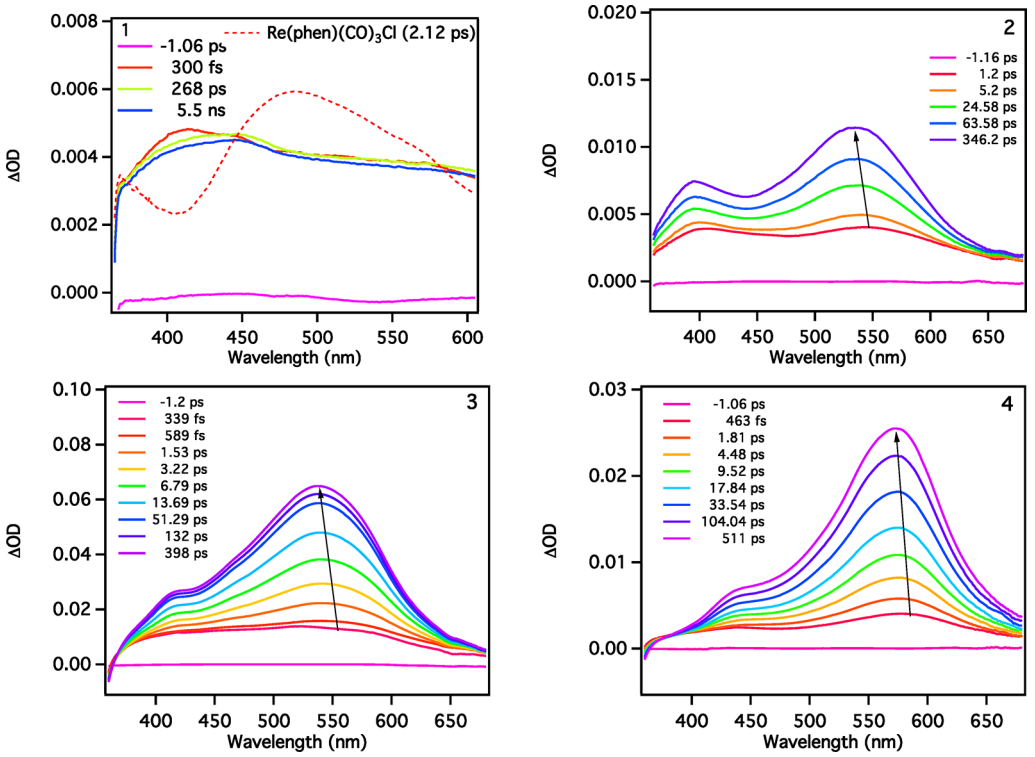


**Figure 5.** Ultrafast TA difference spectra of **1**–**4** recorded in THF. The ultrafast TA difference spectrum of the model chromophore $Re(phen)(CO)_3Cl$ (red dashed line) at 2.12 ps delay is included with **1** for a direct comparison. All difference spectra were obtained using 352 nm excitation (0.4–0.8 mJ $pulse^{-1}$; 90 fs fwhm) with sample o.d.'s of ~0.45.

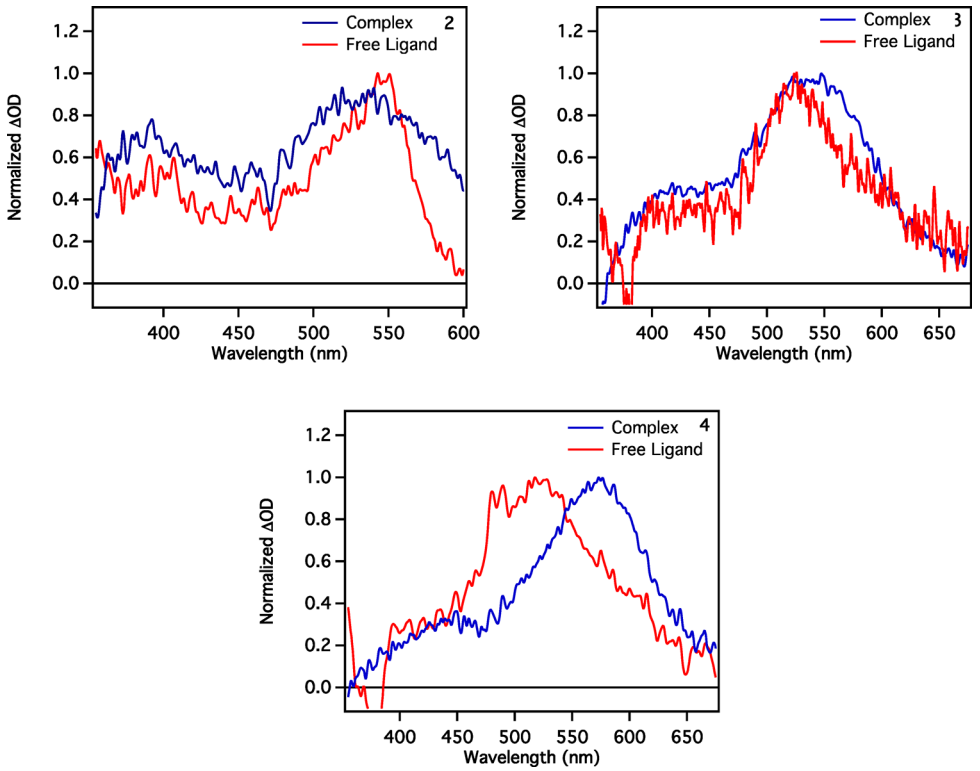


**Figure 6.** Normalized nanosecond sensitized triplet absorption difference spectra (red spectra) of the free isocyanide ligands corresponding to those in molecules **2**–**4** compared to the normalized absorption difference spectra for **2**–**4** measured promptly in nanosecond TA experiments (blue spectra). Excitation was performed at 355 nm (~1.0 mJ $pulse^{-1}$; 7 ns fwhm), and spectra were recorded with 5 $\mu$s delay relative to excitation and 50 ns gate width. The triplet sensitizers were benzophenone for **2** and thioxanthen-9-one for **3** and **4**.



DOI: 10.1021/acs.inorgchem.9b01155
*Inorg. Chem.* XXXX, XXX, XXX–XXX

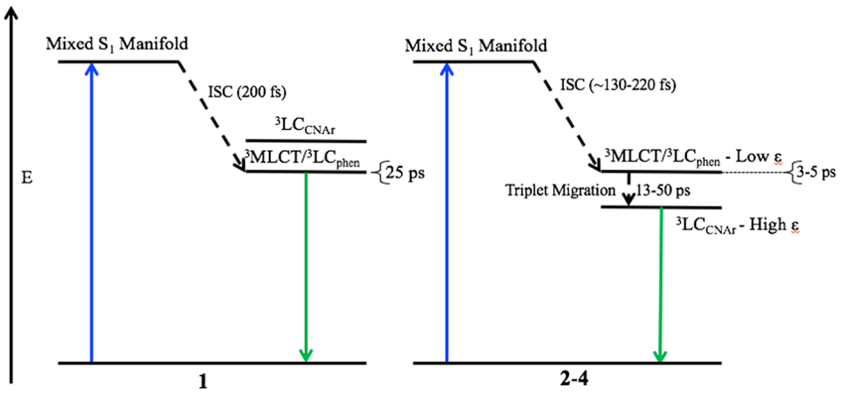


**Figure 7.** Qualitative energy-level diagrams summarizing the photophysical behavior of **1**−**4**.

crossing from the singlet manifold to the configurationally mixed triplet state ($^3$MLCT/$^3$LC) analogous to that assigned in **1**. This is followed by vibrational relaxation within this configurationally mixed triplet excited state that is similar to **1**, now with a slightly faster time constant ranging between 3 and 5 ps. However, after the prompt formation and vibrational cooling of this initially populated state, there is a significantly slower process (ranging from 13 to 50 ps) believed to be triplet migration to an excited state with a significantly higher extinction coefficient, which is also responsible for the substantial absorption growth observed for **2**−**4** in the visible region over this time range.

Because these data are quite distinguishing, we assign the long-lived excited-state absorptions in **2**−**4** to the pure $^3$LC excited states corresponding to the respective isocyanide ligand residents in the structure. Further evidence for these assignments emerges from the sensitized triplet spectra of the free isocyanide ligands resulting from sensitization of **2** with benzophenone and sensitization of **3** and **4** with thioxanthen-9-one (Figure 6). In order to best mimic the Lewis acidic character of the rhenium(I) center, trifluoroacetic acid (TFA) was added to the respective sensitization experiments to singly protonate the relevant isocyanide ligand. Although the positions of the resultant triplet absorbances in the free ligands are somewhat shifted with respect to the TAs observed in the analogous rhenium(I) chromophores, their bandshapes are qualitatively similar and therefore consistent with formation of the $^3$LC excited state on the respective isocyanide moiety. Overall, the combined ultrafast TA data and the nanosecond triplet sensitization experiments suggest triplet energy migration from the initially populated $^3$MLCT/$^3$LC state to the $^3$LC state of the respective isocyanide ligand occurring with time constants of 50, 13.5, and 26 ps in **2**−**4**, respectively. An extensive literature search revealed no related reports of excited-state dynamics occurring between configurationally mixed $^3$MLCT/$^3$LC excited states, with a second $^3$LC excited state located on an ancillary ligand. Clearly, there is ample space for additional investigations in this general area, and many combinations of metal centers and ligands can be conceived to glean further insight into such intramolecular triplet-energy migration processes.

In **1**−**4**, the persistent transient signals from the ultrafast TA experiments measured at long delay times quantitatively match the corresponding nanosecond TA difference spectra, indicating that no significant dynamics are taking place between the 5.5 ns delay time in the ultrafast experiment and 15 ns, the earliest prompt signal resolvable in the nanosecond TA apparatus. The nanosecond TA difference spectra of **1**−**4** as well as their associated transient decay kinetics are provided in Figures S23−S26. The PL and TA decay kinetics measured for **1**−**4** using conventional time-resolved PL and laser flash photolysis experiments were all adequately modeled with single-exponential decays and featured quantitative agreement between both experiments in all instances (Table 2). Consistent with the $^3$MLCT/$^3$LC (phen; in **1**) and $^3$LC (isocyanide; in **2**−**4**) excited-state assignments suggested above, the long-lived excited-state lifetimes recorded here, 8.9, 15.5, 710, and 663 $\delta$s, respectively, are completely congruent with those assignments. Figure 7 presents qualitative Jablonski diagrams of **1**−**4**, summarizing all of the photophysical processes and their corresponding assignments resulting from the current investigation.

**Temperature-Dependent Time-Resolved PL and TA Experiments.** In order to investigate the relative energies of the closely lying triplet excited states featured in this series of molecules, the excited-state decay rates of each chromophore were measured as a function of the temperature. To best fit the series dynamic temperature data, a three-state Boltzmann distribution model was invoked; Figure 8 and eqs 1−3 describe

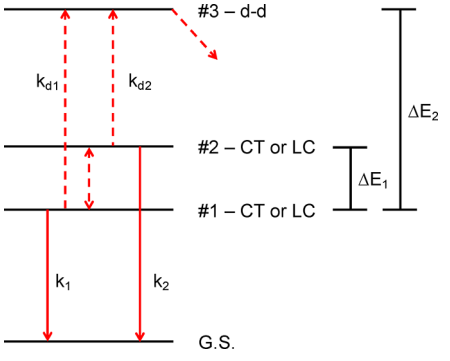


**Figure 8.** Generalized energy-level diagram depicting the parameters of three-state Boltzmann model used to model temperature-dependent excited-state decay in molecules **1**−**4**.

this three-state model.[8,71] The three excited states involved here are defined as two emissive triplet states of charge-transfer and/or LC character and the third of a thermally deactivating metal-centered ligand-field state. This three-state model has been successfully applied to similar rhenium(I) diimine complexes.[8] Consistent with these previous studies, a simple two-state model using one triplet excited state and one d−d


DOI: 10.1021/acs.inorgchem.9b01155
Inorg. Chem. XXXX, XXX, XXX−XXX

state does not adequately fit our data without giving physically unreasonable results.

$$k_{d1} = A_1 e^{-\Delta E_2/kT} \quad (1)$$

$$k_{d2} = A_2 e^{-\Delta E_2 - \Delta E_1/kT} \quad (2)$$

$$\tau = \frac{1}{k_{obs}} = \frac{1 + e^{-\Delta E_1/RT}}{k_1 + k_2 e^{-\Delta E_1/kT} + (A_1 + A_2)e^{-\Delta E_2/kT}} \quad (3)$$

A few assumptions accompany this particular model. The first is that the two lower excited states are photoluminescent. The second is that the upper d−d ligand-field states deactivate so efficiently that, once this state is populated, there are no viable radiative decay pathways. Third, the role of the self-quenching phenomenon noted for complexes **3** and **4** is negated by conducting experiments at low concentrations where self-quenching was not observed. Finally, it is also assumed that $\Delta E_2$ is sufficiently greater than $\Delta E_1$ such that the rates of thermal activation to the ligand-field state can be combined into a single preexponential factor $(A_1 + A_2)$. The most adequate fits taking into account all of the time-resolved temperature-dependent PL (**1** and **2**) or absorbance data (**3** and **4**) for all four complexes are presented in Figure S27, and the values for each relevant fitting parameter are summarized in Table 4.

**Table 4. Summary of Fitting Values from the Three-State Boltzmann Distribution Model**[a]

| complex | $\Delta E_1$[b] | $\Delta E_2$[b] | $k_1$[c] | $k_2$[c] |
|---|---|---|---|---|
| **1** | 545 | 4042 | 9.3 | 53.0 |
| **2** | 496 | 4042 | 3.1 | 55.0 |
| **3** | 775 | 5622 | 0.55 | 22.5 |
| **4** | 806 | 5957 | 0.12 | 25.1 |

[a]The preexponential factor $(A_1 + A_2)$ was fixed to $4 \times 10^{12}$ for **1** and **2**[8] and floated between $4 \times 10^{14}$ and $8 \times 10^{14}$ for **3** and **4**. [b]Units of $cm^{-1}$ [c]Value $\times 10^4$ $s^{-1}$

From the extracted parameters, a number of conclusions can be drawn. In **1** and **2**, the energy gap between the lowest triplet manifold and the d−d state is approximately 4000 $cm^{-1}$, in good agreement with similar molecules modeled in an identical fashion.[8] According to the relative rates of decay from the two emissive excited states, the lower state is consistent with being $^3$LC in character, whereas the higher-lying excited state is more in line with the $^3$CT character. Additionally, the ordering of triplet states is consistent with the TD-DFT modeling of the transitions, where $S_0 \rightarrow T_1$ is LC on the phen ligand and $S_0 \rightarrow T_2$ is the MLCT transition (Figure S13). From a combination of the kinetic and DFT modeling, 77 K PL emission spectra, and conclusions drawn from the TA dynamics, it can be concluded that the lower triplet excited state in **1** is $^3$LC (phen) and the upper excited state is likely $^3$MLCT. Definitive assignments of the lowest $^3$LC state in **2** are more difficult because this molecule likely features a mixed $^3$LC state resulting from the nearly isoenergetic combination of both the phen and the isocyanide triplets. TD-DFT modeling reveals that the energy difference between $S_0 \rightarrow T_1$ (phen) and $S_0 \rightarrow T_2$ (isocyanide) is approximately 0.03 eV (Figure S14). Because these two states are relatively isoenergetic, they could not be distinguished with the use of an additional parameter in the Boltzmann fit, so their relative ordering simply cannot be determined using temperature-dependent PL decay data. However, the RT TA data suggest that the lowest-energy state is most likely $^3$LC (CNAr) in the case of **2**.

Complexes **3** and **4** feature an entirely different series of molecular excited states that are in play. The first obvious difference is that a much larger energy gap between the lowest triplet and ligand-field states now exists, ∼5600−6000 $cm^{-1}$. Additionally, the decay rate from that lowest triplet excited state is significantly slower in comparison to that observed in **1** and **2**. If it is assumed that the differences in the ligand-field state energy between all four molecules are negligible, we can readily conclude that the lower triplet excited states in **3** and **4** are no longer $^3$LC (phen)/$^3$MLCT-based but rather $^3$LC (CNAr)-localized. This is consistent with the combined PL, TA, and electronic structure calculations (Figures S15 and S16), therefore rendering the upper excited state in **3** and **4** using the model presented in Figure 8 as an admixture of nearly isoenergetic $^3$LC(phen)/$^3$MLCT states.

## CONCLUSIONS

This study investigated a series of rhenium(I)-based diiminetricarbonyl arylisocyanide chromophores (**1**−**4**) featuring interactions between three closely lying triplet excited states. The combined experimental evidence illustrated that the CNAr ligand was actively engaged in manipulating excited-state decay in three of these molecules (**2**−**4**), wherein the $^3$MLCT state along with two $^3$LC excited-state configurations (phen and CNAr) conspired to produce the resultant photophysical properties. As the $\pi$ conjugation within the CNAr ligand was extended, the initially generated $^3$LC-(phen)/$^3$MLCT excited state in **1** ultimately migrated to the CNAr $^3$LC state on the order of tens of picoseconds in **2**−**4**. It should be noted that previous literature has described $d\pi(Re)-\pi^*(CNAr)$ $^3$MLCT transitions existing in a number of complexes not featuring a diimine moiety.[35,36] The existence of this transition and any role it may play in the photophysics of the complexes in this current study was considered; however, no spectroscopic computational evidence was found to support this consideration. Chromophores **3** and **4** with RT lifetimes near 700 $\delta$s represent unique examples of excimer formation from inorganic molecules, albeit from interactions between the $^3$LC state and a corresponding ground-state molecule, as evidenced by dynamic self-quenching in the corresponding PL intensity decays, accompanied by the observation of a short-lived low-energy orange-to-red emission feature in both instances. In the quest for generating new classes of molecular-based charge-transfer excited states intended for driving high-energy chemical transformations, all excited configurations must be considered to achieve the proper chromophore design. While $^3$LC excited states on diimine and ancillary ligands are energetically out-of-reach in most visible-absorbing MLCT chromophores, they are quite relevant and can dominate excited-state decay in near-UV-absorbing MLCT molecules, as was observed in **2**−**4** in the present study.

## EXPERIMENTAL SECTION

**General Procedures.** All reagents and solvents used in the synthetic procedures were obtained from commercial sources and used as received, unless otherwise noted. $^1$H and $^{13}$C NMR spectra were recorded on a Varian Innova 400 MHz spectrometer with working frequencies of 400 and 100 MHz for $^1$H and $^{13}$C NMR, respectively. All NMR spectra were plotted and processed using the


DOI: 10.1021/acs.inorgchem.9b01155
Inorg. Chem. XXXX, XXX, XXX−XXX

*MestReNova* software, version 10.0.2. High-resolution ESI-MS data were measured at the Michigan State University Mass Spectrometry and Metabolomics Core (Waters Xevo G2-XS QTOF). Electronic absorption spectroscopic measurements were recorded on a Shimadzu UV-3600 spectrophotometer in 1 cm quartz cuvettes with spectrophotometric-grade THF as the solvent. Steady-state emission measurements were made on an FS-980 fluorimeter (Edinburgh Instruments) fitted with a 450 W xenon arc lamp and a PMT detector in sealable 1 cm quartz cuvettes designed for air-free handling.

**Ultrafast TA Spectroscopy.** Time-resolved TA measurements were performed at the NCSU Imaging and Kinetic Spectroscopy Laboratory in the Department of Chemistry. Subpicosecond absorption transients were detected using a Helios TA spectrometer from Ultrafast Systems. A portion of the output from a 1 kHz Ti:sapphire Coherent Libra regenerative amplifier (4 mJ; 100 fs fwhm at 800 nm) was split into the pump and probe beams. The probe beam was delayed in a 6 ns optical delay stage, while the pump beam was directed into an optical parametric amplifier (Coherent OPerA Solo) to generate tunable excitation. These measurements were performed according to previously published methods.[58,72]

**Nanosecond TA Spectroscopy, Time-Resolved PL, and Time-Gated PL Spectroscopic Measurements.** Nanosecond TA measurements and time-gated PL spectra were collected with a LP920 laser flash photolysis system (Edinburgh Instruments) using, for excitation, a Minilite 355 Nd:YAG (Continuum). TA difference and PL spectra were collected using an iStar ICCD camera (Andor Technology), controlled by the LP900 software (Edinburgh Instruments). Emission decay kinetics were measured using Minilite 355 Nd:YAG (Continuum) excitation and collected using an apparatus described previously.[64] All samples were prepared air-free in a glovebox and sealed in sealable 1 cm quartz cuvettes.

**Triplet Sensitization of Free Ligands.** In order to obtain free-ligand triplet TA spectra, a sensitizer was added (to achieve an o.d. at excitation of ∼0.2) to saturated solutions of the free ligands is THF. All preparation was done air-free in a glovebox. For the phen and isocyanide ligands of **2**, benzophenone was used as the sensitizer and excited at 355 nm. For the isocyanide ligands of **3** and **4**, thioxanthone was used as the sensitizer and excited at 410 nm using the Vibrant 355 Nd:YAG/OPO (OPOTEK). For the spectra of all isocyanide ligands, TFA (∼10%) was added to mimic the Lewis acid effect of complexation.

**DFT Calculations.** The calculations utilized in this study were performed using the *Gaussian 09* software package (revision D.01)[73] and the computation resources of the NCSU High Performance Computing Center. Ground- and triplet-state geometry optimizations were performed using the M06 functional,[74] along with the def2-SVP basis set of Aldrich's group, as implemented in *Gaussian 09*.[75] The Stuttgart−Dresden effective core potentials[76] were used to replace the core electrons in rhenium for all calculations. The PCM was used to simulate the THF solvent environment for all calculations.[77] Frequency calculations were performed on all optimized structures, and no imaginary frequencies were obtained. The TD-DFT calculations were performed using the same conditions as those described for the geometry optimizations.[78−80] The energy and oscillator strengths were computed for each of the 50 lowest singlet excitations and 10 lowest triplet excitations. The natural transition orbitals of the low-lying singlet and triplet transitions were generated using *GaussView 5.0*.[81]

**General Synthetic Procedure for the Re-CNAr Molecules.** This general preparation was adapted from the previously reported synthesis.[13] In a two-necked 100 mL round-bottom flask with a reflux condenser, solid Re(phen)$(CO)_3$Cl and silver triflate (slight excess) were purged with a heavy $N_2$ gas flow. To the solids was added absolute ethanol (25 mL), and the mixture was sealed under $N_2$. The mixture was protected from light and heated to 85 °C for 4 h. The mixture was then filtered hot over Celite. The filter solution was returned to reflux and the appropriate isocyanide ligand was dissolved in a minimal amount of absolute ethanol and added to the reflux reaction via a syringe. After another 4 h. the reaction mixture was cooled and the solvent concentrated to ∼5 mL in vacuo. This concentrated solution was added dropwise to 150 mL of stirring diethyl ether, producing a solid slurry. These solids were filtered and dried to yield the crude product as triflate salt. This solid was dissolved in minimal methanol and recrystallized by the addition of a saturated solution of $NH_4PF_6$ in deionized water. The pure recrystallized solid was filtered, washed with excess deionized water and pentane, and then dried under vacuum.

**[Re(phen)$(CO)_3$(DippCN)]$PF_6$ (1).** Re(phen)$(CO)_3$Cl (340 mg, 0.699 mmol), $AgCF_3SO_3$ (185 mg, 0.720 mmol), and 2,6-diisopropylphenyl isocyanide (132 mg, 0.705 mmol) were used. Yield: 443 mg, 81%. $^1$H NMR (400 MHz, $CD_2Cl_2$): $\delta$ 9.46 (dd, 2H, $J$ = 5.2 and 1.4 Hz), 8.87 (dd, 2H, $J$ = 8.3 and 1.4 Hz), 8.28 (s, 2H), 8.10 (dd, 2H, $J$ = 8.3 and 5.2 Hz), 7.29 (t, 1H, $J$ = 7.9 Hz), 7.03 (d, 2H, $J$ = 7.9 Hz), 2.43 (sep, 2H, $J$ = 6.9 Hz), 0.84 (d, 12H, $J$ = 6.9 Hz). $^{13}$C NMR (100 MHz, $CD_2Cl_2$): $\delta$ 191.5 (2C), 188.3, 155.0 (2C), 147.5, 146.0, 140.1, 132.0, 131.6 (2C), 129.1, 127.6, 124.4, 131.2 (2C), 128.8, 128.6, 128.5, 127.9, 127.8, 126.9, 126.7, 126.1, 125.8, 125.7, 125.4, 30.6, 22.1. HR-MS ([M − $PF_6$]$^+$). Calcd: $m/z$ 636.1425. Found: $m/z$ 636.1426. FTIR (ATR, cm$^{-1}$): 2172 (m), 2035 (s), 1961 (sh), 1925 (s).

**[Re(phen)$(CO)_3$(PhDippCN)]$PF_6$ (2).** Re(phen)$(CO)_3$Cl (340 mg, 0.699 mmol), $AgCF_3SO_3$ (185 mg, 0.720 mmol), and 4-phenyl-2,6-diisopropylphenyl isocyanide (187 mg, 0.710 mmol) were used. Yield: 444 mg, 74%. $^1$H NMR (400 MHz, $CD_2Cl_2$): $\delta$ 9.48 (dd, 2H, $J$ = 5.2 and 1.4 Hz), 8.88 (dd, 2H, $J$ = 8.3 and 1.4 Hz), 8.29 (s, 2H), 8.11 (dd, 2H, $J$ = 8.3 and 5.2 Hz), 7.47−7.36 (m, 5H), 7.23 (s, 2H), 2.49 (sep, 2H, $J$ = 6.9 Hz), 0.89 (d, 12H, $J$ = 6.9 Hz). $^{13}$C NMR (100 MHz, $CD_2Cl_2$): $\delta$ 190.9 (2C), 187.8, 154.4 (3C), 146.9, 145.9, 143.8, 140.2, 139.6, 131.5, 128.9, 128.5, 128.3, 127.1, 127.0, 122.6, 30.2, 21.6. HR-MS ([M − $PF_6$]$^+$). Calcd: $m/z$ 712.1738. Found: $m/z$ 712.1730. FTIR (ATR, cm$^{-1}$): 2174 (m), 2034 (s), 1965 (sh), 1938 (s).

**[Re(phen)$(CO)_3$(PhEthDippCN)]$PF_6$ (3).** Re(phen)$(CO)_3$Cl (340 mg, 0.699 mmol), $AgCF_3SO_3$ (185 mg, 0.720 mmol), and 4-phenylethynyl-2,6-diisopropylphenyl isocyanide (202 mg, 0.703 mmol) were used. Yield: 463 mg, 75%. $^1$H NMR (400 MHz, $CD_2Cl_2$): $\delta$ 9.47 (dd, 2H, $J$ = 5.2 and 1.4 Hz), 8.88 (dd, 2H, $J$ = 8.3 and 1.4 Hz), 8.29 (s, 2H), 8.11 (dd, 2H, $J$ = 8.3 and 5.2 Hz), 7.48 (m, 2H), 7.35 (m, 3H), 7.20 (s, 2H), 2.43 (sep, 2H, $J$ = 6.9 Hz), 0.87 (d, 12H, $J$ = 6.9 Hz). $^{13}$C NMR (100 MHz, $CD_2Cl_2$): $\delta$ 191.3 (2C), 188.2, 155.0 (2C), 147.5, 146.2, 140.8, 132.2, 132.0, 129.6, 129.1, 127.6, 127.5, 126.7, 122.8, 93.0, 88.6, 30.6, 22.0. HR-MS ([M − $PF_6$]$^+$). Calcd: $m/z$ 736.1738. Found: $m/z$ 736.1728. FTIR (ATR, cm$^{-1}$): 2172 (m), 2032 (s), 1959 (sh), 1947 (s).

**[Re(phen)$(CO)_3$(DiPhDippCN)] $PF_6$ (4).** Re(phen)$(CO)_3$Cl (340 mg, 0.699 mmol), $AgCF_3SO_3$ (185 mg, 0.720 mmol), and 4-biphenyl-2,6-diisopropylphenyl isocyanide (240 mg, 0.707 mmol) were used. Yield: 516 mg, 79%. $^1$H NMR (400 MHz, $CD_2Cl_2$): $\delta$ 9.48 (dd, 2H, $J$ = 5.2 and 1.4 Hz), 8.88 (dd, 2H, $J$ = 8.3 and 1.4 Hz), 8.29 (s, 2H), 8.12 (dd, 2H, $J$ = 8.3 and 5.2 Hz), 7.66 (m, 2H), 7.62 (m, 2H), 7.56 (m, 2H), 7.45 (m, 2H), 7.36 (m, 1H), 7.29 (s, 2H), 2.43 (sep, 2H, $J$ = 6.9 Hz), 0.84 (d, 12H, $J$ = 6.9 Hz). $^{13}$C NMR (100 MHz, $CD_2Cl_2$): $\delta$ 191.5 (2C), 188.3, 155.0 (2C), 147.5, 146.5, 143.9, 141.7, 140.8, 140.6, 138.9, 132.0, 129.4, 129.1, 128.3, 128.1, 127.6, 127.5, 123.0 (2C), 30.8, 22.2. HR-MS ([M − $PF_6$]$^+$). Calcd: $m/z$ 788.2051. Found: $m/z$ 788.2136. FTIR (ATR, cm$^{-1}$): 2169 (m), 2035 (s), 1965 (sh), 1932 (s).

## ■ ASSOCIATED CONTENT

### Supporting Information

The Supporting Information is available free of charge on the ACS Publications website at DOI: 10.1021/acs.inorgchem.9b01155.

Additional static and time-resolved spectra, temperature-dependent data, structural characterization data, and DFT calculations for **1**−**4** (PDF)



DOI: 10.1021/acs.inorgchem.9b01155
*Inorg. Chem.* XXXX, XXX, XXX−XXX

## AUTHOR INFORMATION


### Corresponding Author

*E-mail: fncastel@ncsu.edu. Phone: (919) 515-3021.

### ORCID

Felix N. Castellano: 0000-0001-7546-8618


### Notes

The authors declare no competing financial interest.

## ACKNOWLEDGMENTS

This work was supported by the U.S. Department of Energy, Office of Science, Office of Basic Energy Sciences, under Award DE-SC0011979. J.E.Y. was supported by the Air Force Institute of Technology.

## REFERENCES


(1) Wrighton, M.; Morse, D. L. Nature of the lowest excited state in tricarbonylchloro-1,10-phenanthrolinerhenium(I) and related complexes. *J. Am. Chem. Soc.* **1974**, *96*, 998−1003.

(2) Fredericks, S. M.; Luong, J. C.; Wrighton, M. S. Multiple Emissions from Rhenium(I) Complexes: Intraligand and Charge-Transfer Emission from Substituted Metal Carbonyl Cations. *J. Am. Chem. Soc.* **1979**, *101*, 7415−7417.

(3) Giordano, P. J.; Wrighton, M. S. The Nature of the Lowest Excited State in fac-Tricarbonylhalobis(4-phenylpyridine)rhenium(I) and fac-(Tricarbonyl(4,4'-bipyridine)rhenium(I): Emissive Organometallic Complexes in Fluid Solution. *J. Am. Chem. Soc.* **1979**, *101*, 2888−2897.

(4) Smothers, W. K.; Wrighton, M. S. Raman Spectroscopy of Electronic Excited Organometallic Complexes: A Comparison of the Metal to 2,2'-Bipyridine Charge-Transfer State of fac-(2,2'-Bipyridine)tricarbonylhalorhenium and Tris(2,2'-Bripyridine)-ruthenium(II). *J. Am. Chem. Soc.* **1983**, *105*, 1067−1069.

(5) Reitz, G. A.; Demas, J. N.; DeGraff, B. A.; Stephens, E. M. Inter- and Intramolecular Excited-State Interactions of Surfactant-Active Rhenium(I) Photosensitizers. *J. Am. Chem. Soc.* **1988**, *110*, 5051−5059.

(6) Sacksteder, L.; Zipp, A. P.; Brown, E. A.; Streich, J.; Demas, J. N.; DeGraff, B. A. Luminescence Studies of Pyridine a-Diimine Rhenium(I) Tricarbonyl Complexes. *Inorg. Chem.* **1990**, *29*, 4335−4340.

(7) Zipp, A. P.; Sacksteder, L.; Streich, J.; Cook, A.; Demas, J. N.; DeGraff, B. A. Luminescence of Rhenium(I) Complexes with Highly Sterically Hindered a-Diimine Ligands. *Inorg. Chem.* **1993**, *32*, 5629−5632.

(8) Sacksteder, L.; Lee, M.; Demas, J. N.; DeGraff, B. A. Long-Lived, Highly Luminescent Rhenium(I) Complexes as Molecular Probes: Intra- and Intermolecular Excited-State Interactions. *J. Am. Chem. Soc.* **1993**, *115*, 8230−8238.

(9) Leasure, R. M.; Sacksteder, L.; Nesselrodt, D.; Reitz, G. A.; Demas, J. N.; DeGraff, B. A. Excited-State Acid-Base Chemistry of (-Diimine)cyanotricarbonylrhenium(I) Complexes. *Inorg. Chem.* **1991**, *30*, 3722−3728.

(10) Kneas, K. A.; Xu, W.; Demas, J. N.; DeGraff, B. A.; Zipp, A. P. Luminescence-Based Oxygen Sensors: ReL(CO)3Cl and ReL(CO)-3CN Complexes on Copolymer Supports. *J. Fluoresc.* **1998**, *8*, 295−300.

(11) Wallace, L.; Rillema, D. P. Photophysical Properties of Rhenium(I) Tricarbonyl Complexes Containing Alkyl- and Aryl-Substituted Phenanthrolines as Ligands. *Inorg. Chem.* **1993**, *32*, 3836−3843.

(12) Wallace, L.; Jackman, D. C.; Rillema, D. P.; Merkert, J. W. Temperature Dependent Emission Properties of Rhenium(I) Tricarbonyl Complexes Containing Alkyl- and Aryl-Substituted Phenanthrolines as Ligands. *Inorg. Chem.* **1995**, *34*, 5210−5214.

(13) Villegas, J. M.; Stoyanov, S. R.; Huang, W.; Rillema, D. P. Photophysical, Spectroscopic, and Computational Studies of a Series of Re(I) Tricarbonyl Complexes Containing 2,6-Dimethylphenyliso-cyanide and 5- and 6-Derivatized Phenanthroline Ligands. *Inorg. Chem.* **2005**, *44*, 2297−2309.

(14) Striplin, D. R.; Crosby, G. A. Nature of the emitting 3MLCT manifold of rhenium(I)(diimine)(CO)3Cl complexes. *Chem. Phys. Lett.* **1994**, *221*, 426−430.

(15) Striplin, D. R.; Crosby, G. A. Photophysical investigations of rhenium(I)Cl(CO)3(phenanthroline) complexes. *Coord. Chem. Rev.* **2001**, *211*, 163−175.

(16) O' Regan, B.; Graetzel, M. A low-cost, high-efficiency solar cell based on dye-sensitized colloidal TiO2 films. *Nature* **1991**, *353*, 737−740.

(17) Hasselmann, G. M.; Meyer, G. J. Diffusion-Limited Interfacial Electron Transfer wiht Large Apparent Driving Forces. *J. Phys. Chem. B* **1999**, *103*, 7671−7675.

(18) Wang, Y.; Asbury, J. B.; Lian, T. Ultrafast Excited-State Dynamics of Re(CO)3Cl(dcbpy) in Solution and on Nanocrystalline TiO2 and ZrO2 Thin Films. *J. Phys. Chem. A* **2000**, *104*, 4291−4299.

(19) Asbury, J. B.; Hao, E.; Wang, Y.; Lian, T. Bridge Length-Dependent Ultrafast Electron Transfer from Re Polypyridyl Complexes to Nanocrystalline TiO2 Thin Films Studied by Femtosecond Infrared Spectroscopy. *J. Phys. Chem. B* **2000**, *104*, 11957−11964.

(20) Anderson, N. A.; Ai, X.; Chen, D.; Mohler, D. L.; Lian, T. Bridge-Assisted Ultrafast Interfacial Electron Transfer to Nanocrystalline SnO2 Thin Films. *J. Phys. Chem. B* **2003**, *107*, 14231−14239.

(21) Chen, Y.; Liu, W.; Jin, J. S.; Liu, B.; Zou, Z. G.; Zuo, J. L.; You, X. Z. Rhenium(I) tricarbonyl complexes with bispyridine ligands attached to sulfur-rich core: Synthesis, structures and properties. *J. Organomet. Chem.* **2009**, *694*, 763−770.

(22) Veronese, L.; Procopio, E. Q.; De Rossi, F.; Brown, T. M.; Mercandelli, P.; Mussini, P.; D'Alfonso, G.; Panigati, M. New dinuclear hydrido-carbonyl rhenium complexes designed as photo-sensiters in dye-sensitized solar cells. *New J. Chem.* **2016**, *40*, 2910−2919.

(23) Lakowicz, J. R. *Topics in Fluorescence Spectroscopy, Vol 4: Probe Design and Chemical Sensing*; Plenum Press: New York, 1994.

(24) de Silva, A. P.; Gunaratne, H. Q. N.; Gunnlaugsson, T.; Huxley, A. J. M.; McCoy, C. P.; Rademacher, J. T.; Rice, T. E. Signaling Recognition Events with Fluorescent Sensors and Switches. *Chem. Rev.* **1997**, *97*, 1515−1566.

(25) Beer, P. D. Tranisition-Metal Receptor Systems for the Selective Recognition and Sensing of Anionic Guest Species. *Acc. Chem. Res.* **1998**, *31*, 71−80.

(26) Guo, X. Q.; Castellano, F. N.; Li; Lakowicz, J. R. Use of a Long-Lifetime Re(I) Complex in Fluorescence Polarization Immunoassays of High-Molecular-Weight Analytes. *Anal. Chem.* **1998**, *70*, 632−637.

(27) Slone, R. V.; Benkstein, K. D.; Belanger, S.; Hupp, J. T.; Guzei, I. A.; Rheingold, A. L. Luminescent transition-metal-containing cyclophanes ("molecular squares'): Covalent self-assembly, host-guest studies and preliminary nanoporous materials applications. *Coord. Chem. Rev.* **1998**, *171*, 221−243.

(28) Lakowicz, J. R. *Principles of Fluorescence Spectroscopy*, 2nd ed.; Kluwer Academic/Plenum Publishers: New York, 1999.

(29) Sun, S. S.; Lees, A. J. Anion recognition through hydrogen bonding: a simple, yet highly sensitive, luminescent metal-complex receptor. *Chem. Commun.* **2000**, 1687−1688.

(30) Baba, A. I.; Shaw, J. R.; Simon, J. A.; Thummel, R. P.; Schmehl, R. H. The photophysical behavior of d6 complexes having nearly isoenergetic MLCT and ligand localized excited states. *Coord. Chem. Rev.* **1998**, *171*, 43−59.

(31) Caspar, J. V.; Meyer, T. J. Application of the energy gap law to nonradiative, excited-state decay. *J. Phys. Chem.* **1983**, *87*, 952−957.

(32) Kober, E. M.; Caspar, J. V.; Lumpkin, R. S.; Meyer, T. J. Application of the energy gap law to excited-state decay of osmium(II)-polypyridine complexes: calculation of relative non-radiative decay rates from emission spectral profiles. *J. Phys. Chem.* **1986**, *90*, 3722−3734.




DOI: 10.1021/acs.inorgchem.9b01155
*Inorg. Chem.* XXXX, XXX, XXX−XXX

(33) Ko, C.-C.; Cheung, A. W.-Y.; Lo, L. T.-L.; Siu, J. W.-K.; Ng, C.-O.; Yiu, S.-M. Synthesis and photophysical studies of new classes of luminescent isocyano rhenium(I) diimine complexes. *Coord. Chem. Rev.* **2012**, *256*, 1546−1555.
(34) Chu, W.-K.; Wei, X.-G.; Yiu, S.-M.; Ko, C.-C.; Lau, K.-C. Strongly Phosphorescent Neutral Rhenium(I) Isocyanoborato Complexes: Synthesis, Characterization, and Photophysical, Electrochemical, and Computational Studies. *Chem. - Eur. J.* **2015**, *21*, 2603−2612.
(35) Chan, K.-C.; Tong, K.-M.; Cheng, S.-C.; Ng, C.-O.; Yiu, S.-M.; Ko, C.-C. Design of Luminescent Isocyano Rhenium(I) Complexes: Photophysics and Effects of the Ancillary Ligands. *Inorg. Chem.* **2018**, *57*, 13963−13972.
(36) Larsen, C. B.; Wenger, O. S. Photophysics and Photoredox Catalysis of a Homoleptic Rhenium(I) Tris(diisocyanide) Complex. *Inorg. Chem.* **2018**, *57*, 2965−2968.
(37) Hartwig, J. F. *Organotransition Metal Chemistry. From Bonding to Catalysis*, 1st ed.; University Science Books, 2010.
(38) Crabtree, R. H. *The Organometallic Chemistry of the Transition Metals*, 4th ed.; John Wiley & Sons: Hoboken, NJ, 2005.
(39) Yamamoto, Y. Zerovalent transition metal complexes of organic isocyanides. *Coord. Chem. Rev.* **1980**, *32*, 193−233.
(40) Welin, E. R.; Le, C.; Arias-Rotondo, D. M.; McCusker, J. K.; MacMillan, D. W. C. Photosensitized, energy transfer-mediated organometallic catalysis through electronically excited nickel(II). *Science* **2017**, *355*, 380−385.
(41) Shields, B. J.; Kudisch, B.; Scholes, G. D.; Doyle, A. G. Long-Lived Charge-Transfer States of Nickel(II) Aryl Halide Complexes Facilitate Bimolecular Photoinduced Electron Transfer. *J. Am. Chem. Soc.* **2018**, *140*, 3035−3039.
(42) Li, J.; Djurovich, P. I.; Alleyne, B. D.; Yousufuddin, M.; Ho, N. N.; Thomas, J. C.; Peters, J. C.; Bau, R.; Thompson, M. E. Synthetic Control of Excited-State Properties in Cyclometalated Iridium(III) Complexes Using Ancillary Ligands. *Inorg. Chem.* **2005**, *44*, 1713−1727.
(43) Shavaleev, N. M.; Monti, F.; Costa, R. D.; Scopelliti, R.; Bolink, H. J.; Orti, E.; Accorsi, G.; Armaroli, N.; Baranoff, E.; Gratzel, M.; Nazeeruddin, M. K. Bright Blue Phosphorescence from Cationic Bis-Cyclometalated Iridium(III) Isocyanide Complexes. *Inorg. Chem.* **2012**, *51*, 2263−2271.
(44) Maity, A.; Le, Q. L.; Zhu, Z.; Bao, J.; Teets, T. S. Steric and Electronic Influence of Aryl Isocyanides on the Properties of Iridium(III) Cyclometalates. *Inorg. Chem.* **2016**, *55*, 2299−2308.
(45) Na, H.; Maity, A.; Teets, T. S. Bis-cyclometalated iridium complexes with electronically modified aryl isocyanide ancillary ligands. *Dalton Trans.* **2017**, *46*, 5008−5016.
(46) Na, H.; Lai, P. N.; Cañada, L. M.; Teets, T. S. Photoluminescence of Cyclometalated Iridium Complexes in Poly(methylmethacrylate) Films. *Organometallics* **2018**, *37*, 3269−3277.
(47) Sattler, W.; Henling, L. M.; Winkler, J. R.; Gray, H. B. Bespoke Photoreductants: Tungsten Arylisocyanides. *J. Am. Chem. Soc.* **2015**, *137*, 1198−1205.
(48) Sattler, W.; Ener, M. E.; Blakemore, J. D.; Rachford, A. A.; LaBeaume, P. J.; Thackeray, J. W.; Cameron, J. F.; Winkler, J. R.; Gray, H. B. Generation of Powerful Tungsten Reductants by Visible Light Excitation. *J. Am. Chem. Soc.* **2013**, *135*, 10614−10617.
(49) Büldt, L. A.; Guo, X.; Vogel, R.; Prescimone, A.; Wenger, O. S. A Tris(diisocyanide)chromium(0) Complex Is a Luminescenct Analog of Fe(2,2′-Bipyridine)$_3^{2+}$. *J. Am. Chem. Soc.* **2017**, *139*, 985−992.
(50) Hua, F.; Kinayyigit, S.; Rachford, A. A.; Shikhova, E. A.; Goeb, S.; Cable, J. R.; Adams, C. J.; Kirschbaum, K.; Pinkerton, A. A.; Castellano, F. N. Luminescent Charge-Transfer Platinum(II) Metallacycle. *Inorg. Chem.* **2007**, *46*, 8771−8783.
(51) Muro, M. L.; Diring, S.; Wang, X.; Ziessel, R.; Castellano, F. N. Photophysics of the Platinum(II) Terpyridyl Terpyridylacetylide Platform and the Influence of Fe(II) and Zn(II) Coordination. *Inorg. Chem.* **2008**, *47*, 6796−6803.
(52) Watts, R. J.; Crosby, G. A.; Sansregret, J. L. Excited states of transition metal complexes. Spectroscopic measurement of d.pi.*-pi.pi.* interactions in iridium(III) complexes. *Inorg. Chem.* **1972**, *11* (7), 1474−1483.
(53) Connick, W. B.; Geiger, D.; Eisenberg, R. Excited-State Self-Quenching Reactions of Square Planar Platinum(II) Diimine Complexes in Room-Temperature Fluid Solutions. *Inorg. Chem.* **1999**, *38*, 3264−3265.
(54) Fleetham, T.; Huang, L.; Li, J. Tetradentate Platinum Complexes for Efficient and Stable Excimer-Based White OLEDs. *Adv. Funct. Mater.* **2014**, *24*, 6066−6073.
(55) Bachmann, M.; Suter, D.; Blacque, O.; Venkatesan, K. Tunable and Efficient White Light Phosphorescent Emission Based on Single Component N-Heterocyclic Carbene Platinum(II) Complexes. *Inorg. Chem.* **2016**, *55*, 4733−4745.
(56) Suzuki, K.; Kobayashi, A.; Kaneko, S.; Takehira, K.; Yoshihara, T.; Ishida, H.; Shiina, Y.; Oishi, S.; Tobita, S. Reevaluation of absolute luminescence quantum yields of standard solutions using a spectrometer with an integrating sphere and a back-thinned CCD detector. *Phys. Chem. Chem. Phys.* **2009**, *11* (42), 9850−9860.
(57) El Nahhas, A. E.; Consani, C.; Blanco-Rodriguez, A. M.; Lancaster, K. M.; Braem, O.; Cannizzo, A.; Towrie, M.; Clark, I. P.; Záliš, S.; Chergui, M.; Vlček, A., Jr. Ultrafast Excited-State Dynamics of Rhenium(I) Photosensitizers [Re(Cl)(CO)$_3$(N,N)]$^+$ and [Re(imidazole)(CO)$_3$(N,N)]$^+$: Diimine Effects. *Inorg. Chem.* **2011**, *50*, 2932−2943.
(58) Yarnell, J. E.; Deaton, J. C.; McCusker, C. E.; Castellano, F. N. Bidirectional"Ping-Pong" Energy Transfer and 3000-Fold Lifetime Enhancement in a Re(I) Charge Transfer Complex. *Inorg. Chem.* **2011**, *50*, 7820−7830.
(59) Watts, R. J.; Crosby, G. A. A comparison of n$\pi$* interactions in aromatics with d$\pi$* - $\pi\pi$* interactions in iridium(III) complexes. *Chem. Phys. Lett.* **1972**, *13* (6), 619−621.
(60) Pomestchenko, I. E.; Castellano, F. N. Solvent Switching between Charge Transfer and Intraligand Excited States in a Multichromophoric Platinum(II) Complex. *J. Phys. Chem. A* **2004**, *108*, 3485−3492.
(61) Kozlov, D. V.; Tyson, D. S.; Goze, C.; Ziessel, R.; Castellano, F. N. Room Temperature Phosphorescence from Ruthenium(II) Complexes Bearing Pyrenylethynylene Subunits. *Inorg. Chem.* **2004**, *43*, 6083−6092.
(62) Goeb, S.; Rachford, A. A.; Castellano, F. N. Solvent-induced configuration mixing and triplet excited stated inversion exemplified in a Pt(II) complex. *Chem. Commun.* **2008**, *0*, 814−816.
(63) Deaton, J. C.; Castellano, F. N. Archetypal Iridium(III) Compounds for Optoelectronic and Photonic Applications. In *Iridium(III) in Optoelectronic and Photonics Applications*, 1st ed.; Zysman-Colman, E., Ed.; John Wiley and Sons Inc.: Chichester, West Sussex, U.K., 2017; pp 1−69.
(64) Tyson, D. S.; Castellano, F. N. Intramolecular Singlet and Triplet Energy Transfer in a Ruthenium(II) Diimine Complex Containing Multiple Pyrenyl Chromophores. *J. Phys. Chem. A* **1999**, *103*, 10955−10960.
(65) Tyson, D. S.; Bialecki, J.; Castellano, F. N. Ruthenium(II) complex with a notably long excited state lifetime. *Chem. Commun.* **2000**, 2355−2356.
(66) Tyson, D. S.; Henbest, K. B.; Bialecki, J.; Castellano, F. N. Excited State Processes in Ruthenium(II)/Pyrenyl Complexes Displaying Extended Lifetimes. *J. Phys. Chem. A* **2001**, *105*, 8154−8161.
(67) Tyson, D. S.; Luman, C. R.; Zhou, X.; Castellano, F. N. New Ru(II) Chromophores with Extended Excited-State Lifetimes. *Inorg. Chem.* **2001**, *40*, 4063−4071.
(68) Polyansky, D. E.; Danilov, E. O.; Castellano, F. N. Observation of Triplet Intraligand Excited States through Nanosecond Step-Scan Fourier Transform Infrared Spectroscopy. *Inorg. Chem.* **2006**, *45*, 2370−2372.


DOI: 10.1021/acs.inorgchem.9b01155
*Inorg. Chem.* XXXX, XXX, XXX−XXX

(69) McCusker, C. E.; Chakraborty, A.; Castellano, F. N. Excited State Equilibrium Induced Lifetime Extension in a Dinuclear Platinum(II) Complex. *J. Phys. Chem. A* **2014**, *118*, 10391−10399.
(70) Yarnell, J. E.; McCusker, C. E.; Leeds, A. J.; Breaux, J. M.; Castellano, F. N. Exposing the Excited-State Equilibrium in an Ir(III) Bichromophore: A Combined Time Resolved Spectroscopy and Computational Study. *Eur. J. Inorg. Chem.* **2016**, *2016*, 1808−1818.
(71) Allsopp, S. R.; Cox, A.; Kemp, T. J.; Reed, W. J. Inorganic Photophysics in Solution, Part 1. Temperature Activation of Decay Processes in the Luminescence of Tris(2,2'-bipyridine)ruthenium(II) and Tris(1,10-phenanthroline)ruthenium(II) ions. *J. Chem. Soc., Faraday Trans. 1* **1978**, *74*, 1275−1289.
(72) Garakyaraghi, S.; Danilov, E. O.; McCusker, C. E.; Castellano, F. N. Transient Absorption Dynamics of Sterically Congested Cu(I) MLCT Excited States. *J. Phys. Chem. A* **2015**, *119*, 3181−3193.
(73) Frisch, M.; Trucks, G.; Schlegel, H.; Scuseria, G.; Robb, M.; Cheeseman, J.; Scalmani, G.; Barone, V.; Mennucci, B.; Petersson, G.; Nakatsuji, H.; Caricato, M.; Li, X.; Hratchian, H. P.; Izmaylov, A. F.; Bloino, J.; Zheng, G.; Sonnenberg, J. L.; Hada, M.; Ehara, M.; Toyota, K.; Fukuda, R.; Hasegawa, J.; Ishida, M.; Nakajima, T.; Honda, Y.; Kitao, O.; Nakai, H.; Vreven, T.; Montgomery, J. A., Jr.; Peralta, J. E.; Ogliaro, F.; Bearpark, M.; Heyd, J. J.; Brothers, E.; Kudin, K.; Rendell, A.; Burant, J. C.; Iyengar, S. S.; Tomasi, J.; Cossi, J. B.; Bakken, V.; Adamo, C.; Jaramillo, J.; Gomperts, R.; Stratmann, R. E.; Yazyev, O.; Austin, A. J.; Cammi, R.; Pomelli, C.; Ochterski, J. W.; Martin, R. L.; Morokuma, K.; Zakrzewski, V. G.; Voth, G. A.; Salvador, P.; Dannenberg, J. J.; Dapprich, S.; Daniels, A. D.; Farkas, Ö.; Foresman, J. B.; Ortiz, J. V.; Cioslowski, J.; Fox, D. J. *Gaussian 09*, eevision D.01; Gaussian, Inc.: Wallingford, CT, 2009.
(74) Zhao, Y.; Truhlar, D. G. The M06 Suite of Density Functionals for Main Group Thermochemistry, Thermochemical Kinetics, Noncovalent Interactions, Excited States, and Transition Elements: Two New Functionals and Systematic Testing of Four M06-Class Functionals and 12 Other Functionals. *Theor. Chem. Acc.* **2008**, *120*, 215−241.
(75) Weigend, F.; Ahlrichs, R. Balanced Basis Sets of Split Valence, Triple Zeta Valence and Quadruple Zeta Valence Quality for H the Rn: Design and Assessment of Accuracy. *Phys. Chem. Chem. Phys.* **2005**, *7*, 3297−3305.
(76) Andrae, D.; Haeussermann, U.; Dolg, M.; Stoll, H.; Preuss, H. Energy-Adjusted Ab Initio Pseudopotentials for the Second and Third Row Transition Elements. *Theor. Chim. Acta.* **1990**, *77*, 123−141.
(77) Cossi, M.; Scalmani, G.; Rega, N.; Barone, V. New Developments in the Polarizable Continuum Model for Quantum Mechanical and Classical Calculations on Molecules in Solution. *J. Chem. Phys.* **2002**, *117*, 43−54.
(78) Stratmann, R. E.; Scuseria, G. E.; Frisch, M. J. An Efficient Implementation of Time-Dependent Density-Functional Theory for the Calculation of Excitation Energies of Large Molecules. *J. Chem. Phys.* **1998**, *109*, 8218−8224.
(79) Bauernschmitt, R.; Ahlrichs, R. Treatment of Electronic Excitations within the Adiabatic Approximation of Time Dependent Density Functional Theory. *Chem. Phys. Lett.* **1996**, *256*, 454−464.
(80) Casida, M. E.; Jamorski, C.; Casida, K. C.; Salahub, D. R. Molecular Excitation Energies to High-Lying Bound States from Time-Dependent Local Density Approximation Ionization Threshold. *J. Chem. Phys.* **1998**, *108*, 4439−4449.
(81) Dennington, R.; Keith, T.; Millam, J. *Gaussview*, version 5; Semichem Inc.: Shawnee Mission, KS, 2009.


DOI: 10.1021/acs.inorgchem.9b01155
*Inorg. Chem.* XXXX, XXX, XXX−XXX